# Reaction Kinetics of Organic Aerosol Studied by Droplet Assisted Ionization: Enhanced Reactivity in Droplets Relative to Bulk Solution

Yao Zhang, Michael J. Apsokardu, Devan E. Kerecman, Marcel Achtenhagen, Murray V. Johnston\*

Department of Chemistry and Biochemistry, University of Delaware, Newark, DE, 19716

**ABSTRACT:** Droplet Assisted Ionization (DAI) is a relatively new method for online analysis of aerosol droplets that enables measurement of the rate of an aerosol reaction. Here, we used DAI to study the reaction of carbonyl functionalities in secondary organic aerosol (SOA) with Girard's T (GT) reagent, a reaction that can potentially be used to enhance the detection of SOA in online measurements. SOA was produced by  $\alpha$ -pinene ozonolysis. Particulate matter was collected on a filter, extracted, and mixed with GT reagent in water. While the reaction hardly proceeded at all in bulk solution, products were readily observed with DAI when the solution was atomized to produce micron-size droplets. Varying the droplet transit time between the atomizer and mass spectrometer allowed the reaction rate constant to be determined, which was found to be four orders of magnitude faster than what would be expected from bulk solution kinetics. Decreasing the water content of the droplets, either by heating the capillary inlet to the mass spectrometer or by decreasing the relative humidity of the air surrounding the droplets in the transit line from the atomizer to the mass spectrometer enhanced product formation. The results suggest that reaction enhancement occurs at the droplet surface, which is consistent with previous reports of reaction acceleration during mass spectrometric analysis, where a bulk solution is analyzed with an ionization method that produces aerosol droplets.

## INTRODUCTION

Recent studies have suggested that reaction rates in microdroplets can be enhanced by several orders of magnitude over similar processes in bulk solution. For the most part, reaction enhancements have been observed when analyzing bulk solutions with ionization techniques that involve generating charged microdroplets, such as electrospray ionization (ESI), 1,2 nanoESI,3 extractive electrospray ionization (EESI)/microdroplet fusion, 4,5 desorption electrospray ionization (DESI),<sup>6,7</sup> and paper spray (PS).<sup>8,9</sup> Enhanced reactivity has been reported for a variety of processes including Girard reactions of ketones, 6,7 Michael reactions, 6 the reaction between 2,6dichlorophenolindophenol and ascorbic acid, 4 and the Katritzky reaction of pyrylium ions with functionalized amines to give Nsubstituted pyridinium cations.9

In principle, several factors may contribute to the observed reaction enhancements including solvent evaporation, <sup>6,8,10</sup> pH changes accompanying the formation of charged droplets, <sup>2,5,10,11,12</sup> and incomplete solvation of reactants at the airdroplet interface. <sup>3,10,13</sup> Solvent evaporation leads to a higher concentration of reactants which increases the reaction rate for a given reaction rate constant, and the diffusion timescale decreases as the droplet shrinks in size which can enhance the rate of diffusion-limited reactions. In a charged microdroplet environment, the effective pH of the solution can move toward an extreme. For example, the pH in an electrospray droplet was found to be 0.5 whereas the bulk solution had a pH of 3.0.<sup>6</sup> Thus, acid-catalyzed reactions may be enhanced in charged droplets. Droplets also have a higher surface-to-volume ratio than bulk solution, allowing reactions at the air-water interface

to contribute more strongly to the overall reaction rate. Factors that can influence reactions at the air-water interface include surface tension,<sup>5</sup> pH<sup>6,14</sup> and orientation of reactants relative to each other.<sup>13,15</sup> Partially solvated molecules at the air-water interface have an incomplete hydration shell which may lower the activation barrier for reaction relative to molecules having a complete hydration shell in the bulk solution.<sup>10</sup> In this respect, Cooks and coworkers have pointed out that a typical solution phase reaction rate constant can be 6 orders magnitude slower than the corresponding rate constant in the gas phase where little or no solvation exists.<sup>16</sup>

A significant limitation of previous studies is that droplet formation is an integral part of the ionization process, which makes it difficult to decouple processes intrinsic to the droplet environment from those unique to the specific ion source. Here, we use an atomizer to generate aerosol droplets, which are subsequently allowed to undergo reaction under controlled conditions outside the mass spectrometer. At the end of the reaction period, the aerosol is analyzed by online mass spectrometry using droplet assisted ionization (DAI). DAI is a process by which aerosol droplets pass through a temperature-controlled capillary inlet into the mass spectrometer. 17,18 Droplet breakup and charge induction are influenced by the pressure gradient across the capillary and the temperature to which the capillary is heated. 16 Droplet reactivity as a function of e.g. reaction time or droplet water content is studied by varying the conditions in the aerosol reactor while keeping the capillary inlet at room temperature, which minimizes the impact of ionization on the measured droplet reactivity. In this way, we are able to determine the reaction rate constant and compare it to what is known about bulk solution reactivity. The temperature of the capillary inlet is explored as a means of increasing the product yield for applications where the timescale for reaction at room temperature is inconvenient.

The reaction of interest in this study is derivatization by Girard's T (GT) reagent<sup>19</sup> of carbonyl functionalities in secondary organic aerosol (SOA) produced by α-pinene ozonolysis. A substantial fraction of ambient SOA is produced by α-pinene ozonolysis,20,21 and improved methods for online analysis are needed to enable both laboratory and field measurements. In general, SOA is produced by oxidation of volatile organic compounds (VOCs) emitted from biogenic and anthropogenic sources.<sup>22,23</sup> The chemical composition of SOA is highly complex, often encompassing several hundred distinct molecular formulas.<sup>24–27</sup> The products of  $\alpha$ -pinene ozonolysis contain carboxylic acid, ketone, aldehyde, and/or alcohol functional groups.<sup>28</sup> These "monomers" can form dimers, trimers, and tetramers by coupling reactions such as hemiacetal formation, <sup>29,30</sup> aldol condensation<sup>27,31</sup> and esterification.<sup>27,32</sup> Derivatization of α-pinene SOA with GT could selectively target molecules having carbonyl functionalities<sup>19</sup> and also increase the sensitivity of detection owing to the formation of a pre-charged quaternary ammonium ion. 19,33,34 The kinetics and mechanism of GT reactions in bulk solution have been thoroughly studied in the literature.35 Enhanced reactivity in microdroplets was first suggested by the work of Girod et al., who studied GT derivatization of cortisone in a DESI experiment. Subsequently, Laskin and coworkers used nano-DESI for GT derivatization of carbonyls in SOA produced by limonene ozonolysis.<sup>7</sup> Here, we build on this previous work by using DAI to study the reaction in aerosol droplets under controlled conditions to better understand the kinetics and mechanism.

# **EXPERIMENTAL**

Materials. All gas flows were generated from zero air. α-Pinene SOA was generated by mixing 7 ppmv ozone with 1 ppmv α-pinene in a flow tube reactor having a residence time of about ~15 s. Aerosol particles exiting the flow tube reactor (mass concentration ~1000 μg/m³) were collected on a glass microfiber filter (cat. no. 1823-025, GE Healthcare, Piscataway, NJ, USA) for over a time period of several days. The filter was sonicated and extracted three times with optima LC/MS grade acetonitrile (Thermo Fisher Scientific, Swedesboro, NJ). The extraction solutions were combined and filtered through a nylon membrane (cat. no. 176, Thermo Fisher Scientific, Swedesboro, NJ). The final solution was transferred into a 15 mL disposable centrifuge tube (cat. No. 05-539-5, Thermo Fisher Scientific, Swedesboro, NJ). The tube was then purged with an ultra-grade house nitrogen line overnight until dry. SOA was then reconstituted to 0.5 mg/mL with optima LC/MS grade water (Thermo Fisher Scientific, Swedesboro, NJ). Girard's T reagent and ammonium sulfate were purchased from Sigma-Aldrich (St. Louis, MO) and used as received. Pinonaldehyde was synthesized using the procedure described in supporting information.

**Aerosol Generation.** Aerosol droplets were generated from aqueous solutions with an atomizer (model ATM226; TOPAS, Dresden, Germany) and a 1 L/min of house air from Zero Air Generator 737 Series (Aadco Instruments, Cleveland, OH, USA), which removed gas-phase ammonia and organics. In our previous work, these conditions were found to produce a

polydisperse distribution of droplets having diameters in the 1-3  $\mu$ m diameter range. <sup>17</sup> Depending on the experiment being performed, the atomization solution contained SOA (0.25 mg/mL), GT (50  $\mu$ M), and/or ammonium sulfate (50  $\mu$ M) dissolved in water. Preliminary experiments were performed with pinonaldehyde (1 mM) for confirming formation of products from the GT derivatization. The aerosol exiting the atomizer had a number concentration on the order of ~10<sup>6</sup> particles/cm³, a solute mass concentration on the order of ~10<sup>2</sup>  $\mu$ g/m³, and a relative humidity (RH) of ~100%.

**Aerosol Reaction.** Figure 1 shows the experimental setup used in this study. Most experiments were performed with the configuration in Figure 1a. In Figure 1a, the atomizer and mass spectrometer inlet assembly were connected by a 10 mm o.d., 6 mm i.d. reaction tube whose length could be varied between 3 and 170 cm. The entrance to the inlet assembly consisted of a Swagelok tee where two inlet flows (one from the atomizer/connecting tube and the other from makeup air – see below) were combined and sent into the DAI capillary. The droplet reaction time is given by the total transit time from the atomizer to the DAI capillary, which for this study ranged from 0.3 to 3.5 s depending on the length of the connecting tube. The tube and Swagelok assembly were held at room temperature, ~25 °C.

A few experiments were performed with the configuration in Figure 1b to qualitatively study the effect of RH on droplet reactivity. Aerosol from the atomizer was sent through 0, 1 or 2 drying tubes containing molecular sieves (part. no. L-4A812B-IMS, Labsorbents, Park Ridge, IL, USA). The RH of the aerosol exiting the tube assembly was determined by the number of tubes: zero tubes inline gave 98%-100% RH, one tube inline gave ~36% RH, and two tubes in line gave ~16% RH. The RH values reported represent the average of measurements at the beginning and end of each experiment. After exiting the drying tube assembly, the aerosol was sent though a condensation growth chamber (CGC; custom built by Aerosol Dynamics, Inc., Berkeley, CA) to condense water back onto the particles so that the DAI signal response was independent of initial RH. In this device, the aerosol passed through a water-saturated wick encased in three separate temperature regions. The first was a "conditioner" region at 5 °C, followed by a heated "initiator" region at 45 °C, and finally a cooled "moderator" region at 10 °C. This sequence of temperatures exposed particles in the air flow to supersaturated water vapor, which condensed onto the particles and grew them to a final size in the  $\sim$ 1-3  $\mu$ m dia. range, independent of the RH of the aerosol entering the CGC. The total transit time between the atomizer and DAI capillary was  $\sim 3$  s.

**DAI Mass Spectrometry.** Mass spectrometry was performed with a Waters SYNAPT G2-S quadrupole ion mobility time-of-flight mass spectrometer (Waters, Milford, Ma) modified for droplet assisted ionization, as shown in Figure 1c.<sup>17</sup> Since air flow through the atomizer and reactor was 1 L/min

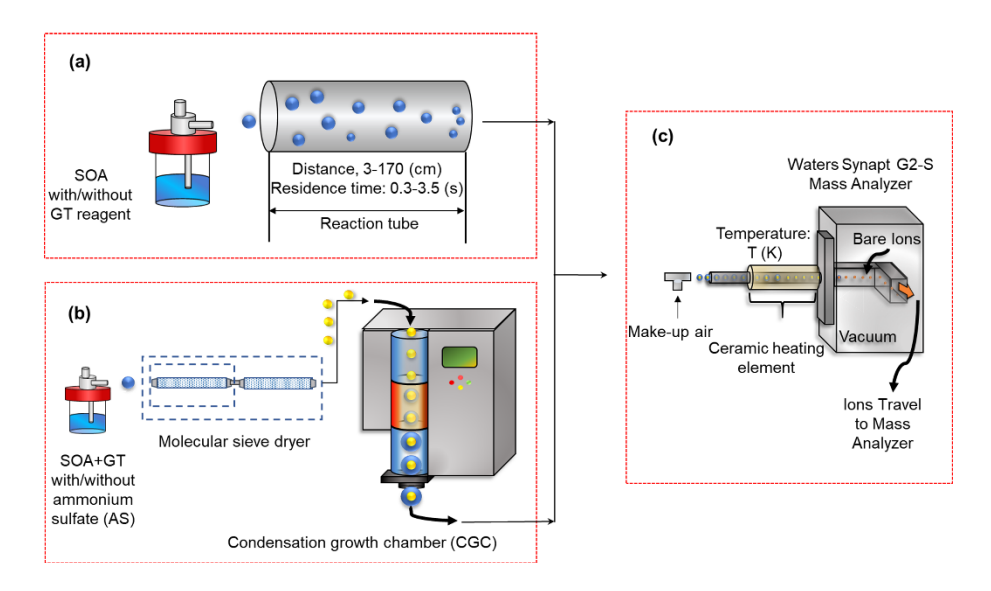


**Figure 1.** Experimental setup for studying aerosol reactions by DAI. The two reaction configurations used in this work are illustrated in (a) and (b). The DAI capillary inlet to the mass spectrometer is illustrated in (c).

and the mass spectrometer sampled air at ~1.3 L/min, an additional ~0.3 L/min of make-up air was added to the air flow through the Swagelok tee at the entrance to the inlet assembly. The inlet consisted of a 62 mm long, 1 mm o.d., 0.5 mm i.d. stainless steel capillary. The first 19 mm of the capillary was unheated, while the remaining portion could be heated up to 850 °C by applying a voltage to 24-gauge NiChrome wire that was encased in a ceramic insulating jacket around the capillary.<sup>17</sup> This assembly is discussed in more detail by Apsokardu et al.<sup>18</sup> Most experiments were performed with the capillary at room temperature. When the capillary was heated above room temperature, the reported temperature was the capillary wall temperature, though the actual temperature that droplets were exposed to in the air flow inside the capillary was likely much lower. For capillary temperature dependence experiment, the transit time from the atomizer to the DAI capillary was  $\sim 1.2$  s, while the temperature applied on the capillary increased from 25 °C to 800 °C. Aerosol transit time through the capillary was ~0.6 ms.

The mass spectrometer was run in sensitivity mode (resolution 10000 FWHM) and continuum mode (continuous signal measurement) for positive and/or negative ion detection as needed. The source temperature was set at 100 °C, cone voltage at 10 V, and offset voltage at 60 V. For DAI-MS/MS experiments, a quadrupole mass filter isolated GT-pinonaldehyde product precursor, with subsequent analysis using collision induced dissociation (CID) with the collision energy adjusted around 12 eV. Spectra were processed as 4 min summations using Waters Masslynx v4.1 software. Peaks in the mass spectra with a relative intensity below 0.5% and an absolute intensity below 5 times the noise were removed from consideration. Background mass spectra were acquired by atomizing pure water

#### RESULTS AND DISCUSSION

**GT Derivatization of Carbonyls in SOA.** GT reacts with carbonyl functional group via two step reaction as shown below (Scheme 1). First, addition of GT to the carbonyl group produces carbinolamine intermediate, followed by the dehydration of water to form a hydrazone. The rate-determining step of Scheme 1 is dependent on the pH of the solution. As the pH decreases from about 5 to 4, the rate determining step changes from the second step to the first. Below a pH of about 4, the hydrazone product is favored. State of the second-order rate constant also increases with decreasing pH. The second-order rate constant also increases with decreasing pH.

## **Scheme 1. GT Reaction Mechanism**

$$\begin{array}{c} O \\ R \\ \end{array} \begin{array}{c} H \\ \end{array} \begin{array}{c} CH_3 \\ H \\ \end{array} \begin{array}{c} O \\ H \\ \end{array} \begin{array}{c} CH_3 \\ H \\ \end{array} \begin{array}{c} O \\ H \\ \end{array} \begin{array}{c} CH_3 \\ H \\ \end{array} \begin{array}{c} O \\ H \\ \end{array} \begin{array}{c} CH_3 \\ H \\ \end{array} \begin{array}{c} O \\ H \\ \end{array} \begin{array}{c} CH_3 \\ H \\ \end{array} \begin{array}{c} O \\ CH_3 \\ \oplus CH_3 \end{array} \end{array}$$

The reaction is first demonstrated by mixing GT reagent with pinonaldehyde, a product of  $\alpha$ -pinene ozonolysis that is produced in high yield. Figure 2 shows (a) the mass spectrum obtained from DAI of GT + pinonaldehyde and (b) the MS/MS spectrum of the GT-pinonaldehyde product, which gives an example what is expected from the GT reaction. The DAI mass spectrum contains a product peak at 282.2 m/z that corresponds to the formula  $C_{15}H_{28}O_2N_3$ , which is the final hydrazone product in Scheme 1 for pinonaldehyde. The observation of just the final hydrazone product suggests that the pH of the droplet is low. Stachissini et al. <sup>35</sup> pointed out for the reaction between benzaldehyde and GT reagent, that hydrazone product formation became favored at a pH of about 4 and below. Figure 2b shows the MS/MS spectrum of the precursor ion at 282.2 m/z. Loss of

trimethylamine produces the fragment ion at 60.1 m/z and 223.1 m/z, further elimination of CO produces the fragment ion detected at 195.1 m/z. Loss of trimethylamine and cross-ring cleavage gives rise to the product ion at 125.1 m/z.

Molecular species in SOA are generally detected as [M+H]<sup>+</sup>, [M+Na]<sup>+</sup>, and/or [M-H]<sup>-</sup>. When derivatized with GT, the products are observed in the positive ion spectrum. Thus, formation of the final hydrazone product results in an m/z increase of either 113.0947 (GT-H-H<sub>2</sub>O) and/or 91.1128 (GT-Na-H<sub>2</sub>O) compared with underivatized peaks in positive mode or 115.1104 (GT+H-H<sub>2</sub>O) compared with underivatized in negative mode.

Figure 3 shows positive ion mass spectra of SOA taken under

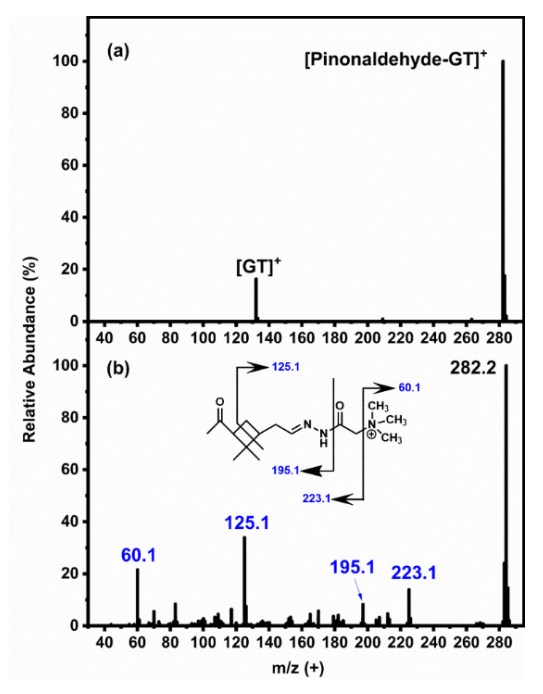


**Figure 2.** Mass spectra of GT derivatized pinonaldehyde. (a) DAI-mass spectrum (+) obtained from atomization of solution with 50  $\mu$ M GT and 1 mM pinonaldehyde and (b) DAI-MS/MS (+) spectrum obtained from GT-pinonaldehyde product.

different conditions. Figure 3a is the DAI mass spectrum of droplets produced by atomization of a solution of SOA in water. Monomers (for the purpose of this study defined as molecules having 10 or fewer carbon atoms), dimers (defined here as molecules having between 11 and 20 carbon atoms), trimers (defined here as molecules having between 21 and 30 carbon atoms) are observed. Most peaks in the positive ion spectrum are sodium cationized. The sodium contamination most likely comes from glass surfaces in the atomizer and/or CGC.

Figure 3b is the DAI mass spectrum of droplets containing SOA and GT. Though obtained under the same DAI conditions as Figure 3a, the ions detected are totally different. Ions highlighted in red have molecular formulas consistent with GT derivatization. The ion highlighted in blue is unreacted GT reagent at 132.1 *m/z*. Ions from unreacted SOA molecules are detected, but the signal intensities are very low, indicating that the GT reagent and GT derivatives cause substantial signal quenching of the unreacted SOA peaks. Signal quenching by GT and its

reaction products was also reported by Laskin et al. who studied GT derivatization of limonene SOA by nano-DESI. With both DAI and nano-DESI, charged derivatives generally ionize more readily than the uncharged percursors. Given the existence of SOA reactant ion signal suppression, a useful measure of the extent of reaction is the ratio of the summed total signal intensities of the product ions (P) divided by the intensity of the GT reagent ion. For the mass spectrum in Figure 3b, the P/GT signal intensity ratio is 13.

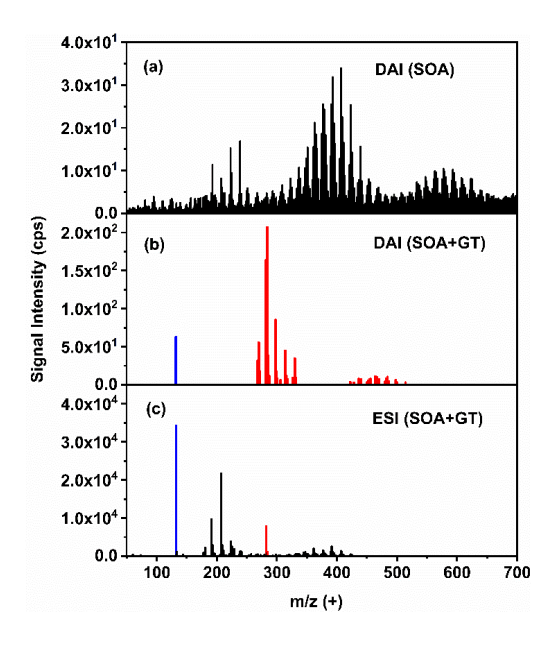


**Figure 3.** (a) DAI mass spectrum (+) of droplets produced by atomization of 0.25 mg/mL  $\alpha$ -pinene SOA in water. (b) DAI mass spectrum (+) of droplets produced by atomization of a solution containing 0.25 mg/mL SOA and 50  $\mu$ M GT in water. (c) ESI (+) mass spectrum of the solution containing SOA and GT in water. Temperature of capillary inlet for DAI: 25 °C. Ions corresponding to the products of the GT reaction are highlighted in red. Unreacted GT is highlighted in blue.

The DAI mass spectrum in Figure 3b was obtained with a capillary wall temperature of 25 °C. At this temperature, most of the reaction occurs in the connecting tube since the droplet transit time through the capillary is short by comparison. This assumption was checked experimentally by performing a control experiment where a pipet tip was positioned just outside the capillary entrance so that droplets could be pulled from the tip directly into the capillary with minimal transit time. The experimental setup is shown in Figure S1, and the mass spectrum obtained from this experiment is shown in Figure S2. Relative to the mass spectrum in Figure 3b where P/GT=13, the DAI-pipet mass spectrum in Figure S2 shows hardly any product formation (P/GT=0.2), confirming that virtually all of the reaction in the Figure 3b experiment occurred in the transfer line rather than inside or beyond the capillary.

This assumption was further checked by electrospray ionization (ESI). Figure 3c is an ESI mass spectrum of the solution used to generate the droplets for the experiment in Figure 3b. The amount of SOA reacted is much less than that in Figure 3b

(P/GT=0.3 for the mass spectrum Figure 3c), which is not surprising since the transit time between droplet formation and sampling in the ESI source is only about 0.6 ms, while it is much longer in the DAI experiment (1.2 s for the mass spectra in both Figure 3a and Figure 3b). The mass spectra in Figures S2 and 3c also highlight that the reaction effectively stops when bare molecular ions are formed from partially desolvated droplets within the mass spectrometer inlet, as reported previously by Bain<sup>1</sup> in an ESI-MS experiment and Lee<sup>4</sup> in a droplet fusion experiment.

Product ions detected in Figure 3b are listed in Table S1 along with the corresponding elemental formulas and in some cases proposed molecular structures of the underivatized carbonyls. Thirty-six formulas were assigned within 5 ppm for product peaks in the monomer and dimer range. Four of the most intense peaks in Figure 3b and their MS/MS spectra correspond to known monomer products of α-pinene ozonolysis containing an aldehyde group (pinalic acid, pinonaldehyde, norpinalic acid, norpinonaldehyde). 37-40 The fraction of product peaks from dimers is fewer than the product peaks from monomers, which may be due to the characteristics of oligomerization reactions expected to occur in SOA. For example, aldehydes can react with alcohols to form hemiacetals/hemiacetals, <sup>29,30</sup> with carbonyls to form aldol,27 and with stabilized Criegee intermediates (SCIs) to form secondary ozonides,<sup>41</sup> all of which remove the aldehyde group from the dimer product.

**Reaction Rate Constant.** To determine the reaction rate constant, experiments with various connecting tube lengths were performed. As indicated by Figures S2 and 3c, hardly any product formation occurs inside the DAI capillary when the wall temperature is set to 25 °C. Therefore, the droplet reaction time is given by the transit time from the atomizer to the DAI capillary. Before we derive the reaction rate constant, we first need to know an approximate concentration of aldehyde/ketone in the SOA solution. It is reported that the concentration of carbonyl functional groups in α-pinene SOA is ~4 μmol/mg, determined by a spectrophotometric derivatization method. According to this result, there is ~1100 μM carbonyl functional groups in the 0.25 mg/mL SOA solution available for reaction. Since carbonyls are in excess when mixed with 50 μM GT, the reaction is assumed to be pseudo-first order in GT:

$$\frac{P_t}{GT_t} = e^{k_{\parallel}t} - 1 \tag{1}$$

$$k_{\rm I} = k_{\rm II}[SOA\ Carbonyls]$$
 (2)

where GT = Girard's T reagent concentration, P = derivatization product concentration,  $k_I$  is the pseudo-first order rate constant,  $k_I$  is the second order rate constant. The plot in Figure 4 is for the ratio of the sum of all product ion intensities divided by the reagent ion intensity, which is proportional to the ratio of the concentrations. The assumption here is that the ionization efficiency of  $[GT]^+$  is the same as  $[M+GT-H_2O]^+$  products. Using Equation 1 to fit the data in Figure 4, gives an average first order rate constant of  $1.43 \pm 0.01 \text{ s}^{-1}$ , which corresponds to a second order reaction rate constant of  $1296 \pm FF 38 \text{ M}^{-1}\text{s}^{-1}$  based on the bulk solution concentrations of SOA carbonyls. Uncertainty in the reaction rate constant is obtained from propagation of standard error of the slope and replicate experiments. In contrast, the second-order reaction rate constant of various carbonyls in bulk

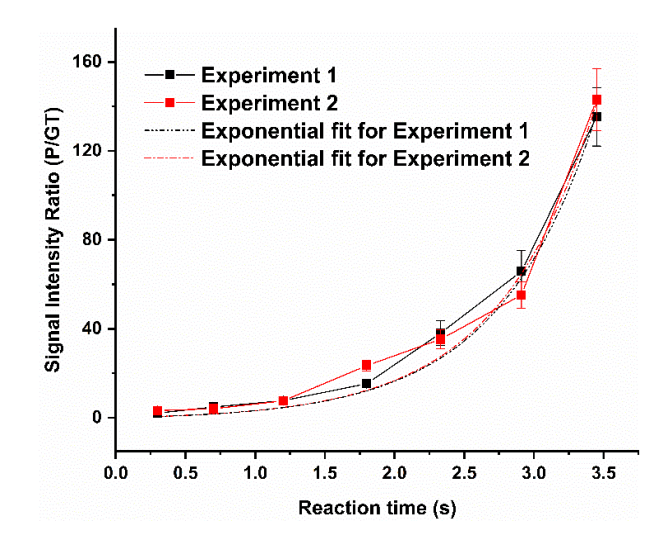


**Figure 4.** P/GT signal intensity ratio vs reaction time for DAI (+) analysis of droplets containing 0.25 mg/mL SOA + 50  $\mu$ M GT. Results are shown for two separate experiments. Exponential fits are described in the text. Error bars represent one standard deviation of the signal intensity ratio.

solution is reported to be on the order of 0.1 M<sup>-1</sup>s<sup>-1</sup> for GT reaction at pH of 4.7, which is the pH of SOA + GT bulk solution used in this experiment, as measured with pH meter.<sup>35</sup> By this reasoning, the average second-order rate constant for SOA carbonyls in droplets is four orders of magnitude greater than that previously reported in bulk solution under comparable reaction conditions. Alternatively, it is possible that the reactants become highly concentrated in the droplet experiment (see discussion below). By this reasoning, the SOA carbonyl concentration in droplets is four orders of magnitude larger than that in bulk solution concentration at most, making the pseudo-first order rate constant much higher than expected. It is also possible that both cases happen at the same time, the increase of the observed reaction rate is a result of combination of these two factors.

Capillary Temperature Dependence. Changing the temperature of the DAI capillary provides the opportunity to qualitatively study the temperature dependence of the reaction for the purpose of enhancing product formation. We anticipate using the Girard T reaction for online detection of carbonyls in SOA through a droplet fusion experiment where droplets containing reagent are produced by electrospray and then allowed to fuse with SOA particles. Based on the data in Figure 4, the relatively long reaction times needed for optimum product formation is disadvantageous since, while the ratio of product to reactant increases with reaction time, the absolute signal intensity decreases owing to wall loss. A potential solution to this problem is to increase the capillary wall temperature to enhance product formation.

Increasing the capillary wall temperature has two advantageous effects. First, Figure 5a shows that the total signal intensity (product plus reagent ion intensities) increases with increasing temperature. Second, Figure 5b shows that the signal intensity ratio of product to reagent ion also increases with increasing temperature. This combination of effects (increasing absolute signal intensity and product formation) means that the sensitivity of product detection is greatly increased when using higher capillary temperatures.

This enhancement should be of great use in organic aerosol studies where the mass flow of aerosol into the mass spectrometer is small.

Increasing absolute intensity has been observed in previous DAI studies and is attributed to an increased efficiency of droplet charging prior to molecular ion ejection. <sup>17,18</sup> As in these previous studies, the absolute signal intensity in Figure 5a is relatively independent of capillary wall temperature below about 300 °C. Droplet charging appears to be inhibited by slow evaporation of water in

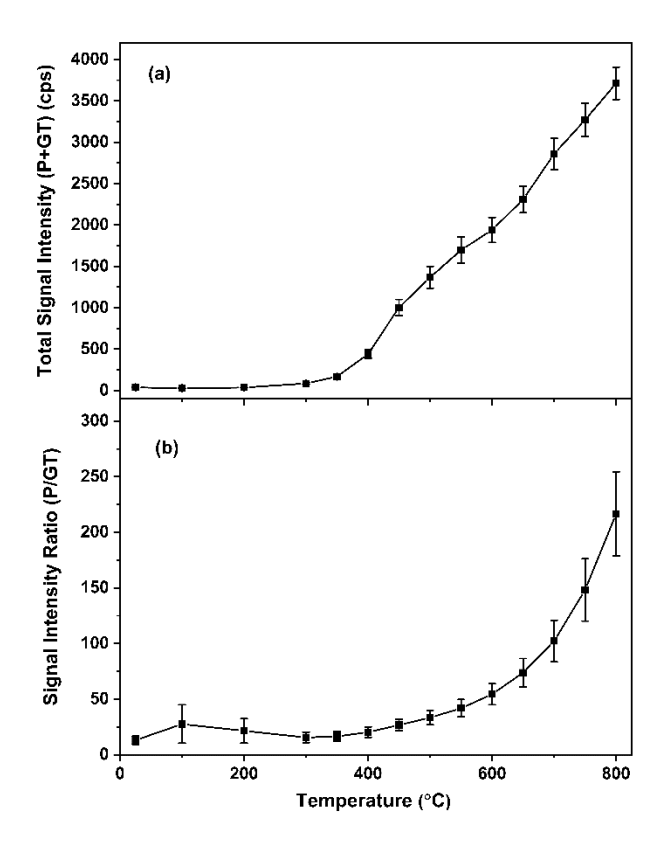


**Figure 5.** a) Plot of total signal intensity (P+GT) as a function of capillary wall temperature. b) Plot of P/GT signal intensity ratio vs. capillary wall temperature. Error bars represent propagation of error from replicate experiments.

this temperature range. <sup>18</sup> The increasing P/GT ratio with increasing temperature may arise from a combination of fast evaporation of water, which would enhance hydrazone product formation, and increased droplet charging, which could lower the droplet pH and thereby favor hydrazone product formation. These possibilities are discussed in more detail in the next section.

**Reaction Mechanism.** Figure 5b suggests that, at least for the region inside the capillary, removing water from the droplets enhances product formation. To qualitatively confirm that this is also true in the transfer line at room temperature, we performed an additional set of experiments where drying tubes were inserted into the transfer line assembly to lower the relative humidity (RH) of the surrounding air and thereby decrease the water content of the droplets. The experimental setup is shown in Figure 1b. To assure that the loss of water from droplets in the air flow from the atomizer to the capillary did not affect DAI detection sensitivities of the products and reactants, a condensation growth chamber was inserted just before the

DAI capillary. In this way, the water content of droplets entering the capillary was independent of the RH coming out of the diffusion driers. The results are shown in Figure 6. In experiments both with and without ammonium sulfate, decreasing the RH had the effect of increasing the product to reactant signal intensity ratio. It is not possible to develop a quantitative relationship between droplet water content (as given by RH) and

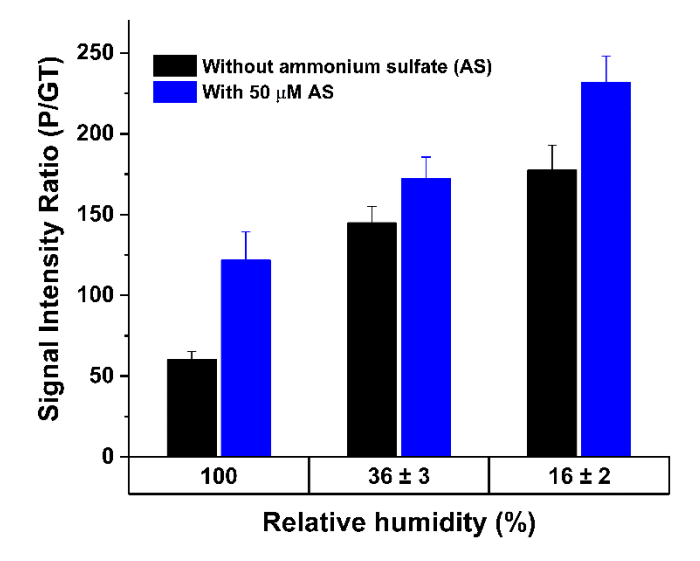


**Figure 6.** The DAI signal intensity ratio of products (P) to reactant (GT) vs. relative humidity (RH) after the diffusion drier(s). All solutions contained 0.25 mg/mL SOA + 50  $\mu$ M GT in water. Error bars represent propagation of error from replicate experiments.

reaction rate from the data in Figure 6, because the RH varies substantially along the reaction path and is measured in only one specific location. Nonetheless, Figures 5 and 6 together suggest that removing water, either by heating the droplets or lowering the RH of the air surrounding them, enhances the formation of product.

One consequence of removing water from the droplets is concentrating the reactants, which could result in a substantial enhancement of the reaction rate. Pure ammonium sulfate provides a helpful example. If droplets produced from a 50 μM ammonium sulfate solution are exposed to air at 90% RH at room temperature, water leaves the droplets and the equilibrium concentration increases to about 4 M. 43 A subsequent decrease of RH will increase the concentration, but by a much smaller amount until efflorescence occurs around 40% RH which corresponds to a concentration of about 20 M.43 While concentration increases of this magnitude could lead to the observed enhancement of the pseudo-first order reaction rate constant between carbonyls and GT reagent, other factors may limit the amount of concentration achieved such as the timescale of the reaction relative to the time to reach equilibrium and the limiting solubilities of GT reagent and SOA carbonyls in water. Furthermore, in experiments performed without drying tubes, the RH we measured was in the 98%-100% range, which makes it unlikely that the observed reaction rate enhancement in the connecting line at room temperature was achieved by concentration of the reactants alone.

An alternative explanation for enhanced product formation with increasing temperature and decreasing water content inside the inlet is the possibility of reaction at the air-water interface. As water evaporates by drying and heating, the surface-to-volume ratio increases. This favors reactions that proceed faster at the air-droplet interface than in bulk solution.<sup>3,13,44</sup> Molecular organization and orientation of reactants could be influenced at air-water interface, <sup>13,15,45</sup> which further results in the change of activation barrier for reaction.<sup>10</sup> If reaction at the interface is fast, the overall second-order rate constant could be much greater in droplets than bulk solution since the diffusion time-scale within the droplet is short (~3x10<sup>-5</sup> s).

Because SOA often coexists with inorganic salts in the atmosphere, the influence of ammonium sulfate on product formation was investigated for a capillary temperature of 25 °C. As Figure 6 shows, ammonium sulfate has the general effect of enhancing product formation. Two possible reasons for this enhancement are pH lowering and "salting out" of reactants. Ammonium sulfate is a weak acid and may assist the acid-catalyzed second step of the reaction sequence (R1). The pH of the SOA-GT bulk solution was ~4.7 while that of the solution with ammonium sulfate added was ~4.4. While this difference is small, it could increase the product-to-reactant ratio since the reaction rate increases with decreasing pH.

In experiments where highly charged droplets are formed, the pH of the microdroplet has been found to be drastically lower than the bulk solution. <sup>2,5,6,8,10</sup> In our experiment, droplet charging occurs in the capillary inlet, so it is possible that successive iterations of solvent evaporation and Coulomb fission could increase the proton density and thereby continuously lower the pH of the droplet.<sup>2,5,11,12,46</sup> However, very little product formation occurs inside the capillary at 25 °C, so fission-induced pH lowering is unlikely. On the other hand, evaporation of ammonia from the droplets may occur in the transfer line, which would decrease the pH when ammonium sulfate was added in the solution and thereby enhance product formation. When higher capillary wall temperatures are used, it is possible that increased droplet charging, as indicated by the total ion signal intensity increase in Figure 5a, does lead to pH lowering and enhanced product formation.

A second possibility is "salting out" of reactants. Salting out refers to the observation that some  $\alpha$ -pinene-derived oxidation products exhibit enhanced surface activity in the presence of ammonium sulfate owing to decreased solubility with the addition of inorganic salt.<sup>47</sup> Therefore, the increase in product formation caused by the addition of ammonium sulfate (Figure 5) could be interpreted as an increase in the surface reaction rate caused by a higher reactant concentration at the air-water interface.

## **CONCLUSIONS**

In this work, DAI was used to determine the rate constant and activation energy for SOA carbonyl derivatization by Girard's T reagent. At room temperature, the reaction rate is shown to be four-orders of magnitude larger than the comparable reaction in bulk solution. Two separate effects may explain this increase: concentration of the reactants as water evaporates from the droplets, and fast reaction at the air-water interface relative to the bulk solution. Water evaporation, either by heating the droplets in the capillary inlet or drying the air surrounding the

droplets in the transfer line, enhances product formation. This suggests that fast reaction at the air-water interface appears to be the major contributor to rate enhancement in microdroplets. Since the Girard's T derivatization reaction requires loss of water to give a final product, it is reasonable to expect that the reaction proceeds more quickly in the partially solvated environment of the air-water interface. In the future, this hypothesis could be tested by analyzing size-selected droplets. Several accretion reactions important to SOA formation also involve elimination of water as the final step and may proceed more quickly at the air-water interface than in bulk solution. Reactions such as these will be the focus of future studies of reaction rate enhancement in droplets.

## ASSOCIATED CONTENT

## **Supporting Information**

Table of GT reaction products detected from  $\alpha$ -pinene SOA. Experimental setup and mass spectrum from the DAI-pipet experiment. Synthesis procedure and NMR spectra for pinonaldehyde.

#### **AUTHOR INFORMATION**

## **Corresponding Author**

Murray V. Johnston - Department of Chemistry and Biochemistry, University of Delaware, Newark, Delaware, 19716, United States; Phone: 302-831-8014; Email: myj@udel.edu

#### **Authors**

Yao Zhang - Department of Chemistry and Biochemistry, University of Delaware, Newark, Delaware, 19716, United States

Michael J. Apsokardu - Department of Chemistry and Biochemistry, University of Delaware, Newark, Delaware, 19716, United States

**Devan E. Kerecman -** Department of Chemistry and Biochemistry, University of Delaware, Newark, Delaware, 19716, United States

Marcel Achtenhagen - Department of Chemistry and Biochemistry, University of Delaware, Newark, Delaware, 19716, United States

## ACKNOWLEDGMENT

This research was supported by the U. S. National Science Foundation under grant number CHE-1904765.

#### **REFERENCES**

- Bain, R. M.; Pulliam, C. J.; Cooks, R. G. Chemical Science Accelerated Hantzsch Electrospray Synthesis with Temporal Control of Reaction Intermediates †. 2015, 397–401.
- (2) Banerjee, S.; Zare, R. N. Syntheses of Isoquinoline and Substituted Quinolines in Charged Microdroplets. *Angew. Chemie - Int. Ed.* 2015, 54, 14795–14799.
- (3) Bain, R. M.; Sathyamoorthi, S.; Zare, R. N. "On-Droplet" Chemistry: The Cycloaddition of Diethyl Azodicarboxylate and Quadricyclane. *Angew. Chemie Int.*

- Ed. 2017, 56, 15083-15087.
- (4) Lee, J. K.; Kim, S.; Nam, H. G.; Zare, R. N. Microdroplet Fusion Mass Spectrometry for Fast Reaction Kinetics. *Proc. Natl. Acad. Sci.* 2015, 112, 3898–3903.
- (5) Lee, J. K.; Banerjee, S.; Nam, H. G.; Zare, R. N. Acceleration of Reaction in Charged Microdroplets. Q. Rev. Biophys. 2015, 48, 437–444.
- (6) Girod, M.; Moyano, E.; Campbell, D. I.; Cooks, R. G. Accelerated Bimolecular Reactions in Microdroplets Studied by Desorption Electrospray Ionization Mass Spectrometry. Chem. Sci. 2011, 2, 501–510.
- (7) Laskin, J.; Eckert, P. A.; Roach, P. J.; Heath, B. S.; Nizkorodov, S. A.; Laskin, A. Chemical Analysis of Complex Organic Mixtures Using Reactive Nanospray Desorption Electrospray Ionization Mass Spectrometry. *Anal. Chem.* 2012, 84, 7179–7187.
- (8) Bain, R. M.; Pulliam, C. J.; Raab, S. A.; Cooks, R. G. Chemical Synthesis Accelerated by Paper Spray: The Haloform Reaction. J. Chem. Educ. 2016, 93, 340–344.
- (9) Yan, X.; Augusti, R.; Li, X.; Cooks, R. G. Chemical Reactivity Assessment Using Reactive Paper Spray Ionization Mass Spectrometry: The Katritzky Reaction. Chempluschem 2013, 78, 1142–1148.
- (10) Yan, X.; Bain, R. M.; Cooks, R. G. Organic Reactions in Microdroplets: Reaction Acceleration Revealed by Mass Spectrometry. Angew. Chemie Int. Ed. 2016, 55, 12960– 12972.
- (11) Gatlin, C. L.; Tureček, F. Acidity Determination in Droplets Formed by Electrospraying Methanol-Water Solutions. Anal. Chem. 1994, 66, 712–718.
- (12) Fenn, J. B. Ion Formation from Charged Droplets: Roles of Geometry, Energy, and Time. J. Am. Soc. Mass Spectrom. 1993, 4, 524–535.
- (13) Nam, I.; Lee, J. K.; Nam, H. G.; Zare, R. N. Abiotic Production of Sugar Phosphates and Uridine Ribonucleoside in Aqueous Microdroplets. *Proc. Natl. Acad. Sci.* **2017**, *114*, 12396–12400.
- (14) Vaida, V. Prebiotic Phosphorylation Enabled by Microdroplets. Proc. Natl. Acad. Sci. 2017, 114, 12359– 12361.
- (15) Chen, X.; Minofar, B.; Jungwirth, P.; Allen, H. C. Interfacial Molecular Organization at Aqueous Solution Surfaces of Atmospherically Relevant Dimethyl Sulfoxide and Methanesulfonic Acid Using Sum Frequency Spectroscopy and Molecular Dynamics Simulation. J. Phys. Chem. B 2010, 114, 15546–15553.
- (16) Cooks, R. G.; Yan, X. Mass Spectrometry for Synthesis and Analysis. *Annu. Rev. Anal. Chem.* **2018**, *11*, 28.
- (17) Horan, A. J.; Apsokardu, M. J.; Johnston, M. V. Droplet Assisted Inlet Ionization for Online Analysis of Airborne Nanoparticles. *Anal. Chem.* 2017, 89, 1059–1062.
- (18) Apsokardu, M. J.; Kerecman, D. E.; Johnston, M. V. Ion Formation in Droplet-Assisted Ionization. *Rapid Commun. Mass Spectrom.* 1–7.
- (19) Wheeler, O. H. The Girard Reagents. *Chem. Rev.* **1962**, 62, 205–221.
- (20) Hallquist, M.; Wenger, J. C.; Baltensperger, U.; Rudich, Y.; Simpson, D.; Claeys, M.; Dommen, J.; Donahue, N. M.; George, C.; Goldstein, A. H.; Hamilton, J. F.; Herrmann, H.; Hoffmann, T.; Iinuma, Y.; Jang, M.; Jenkin, M. E.; Jimenez, J. L.; Kiendler-Scharr, A.; Maenhaut, W.; McFiggans, G.; Mentel, T. F.; Monod, A.; Prévôt, A. S. H.; Seinfeld, J. H.; Surratt, J. D.; Szmigielski, R.; Wildt, J. The Formation, Properties and Impact of

- Secondary Organic Aerosol: Current and Emerging Issues. *Atmos. Chem. Phys.* **2009**, *9*, 5155–5236.
- (21) Shrivastava, M.; Cappa, C. D.; Fan, J.; Goldstein, A. H.; Guenther, A. B.; Jimenez, J. L.; Kuang, C.; Laskin, A.; Martin, S. T.; Ng, N. L.; Petaja, T.; Pierce, J. R.; Rasch, P. J.; Roldin, P.; Seinfeld, J. H.; Shilling, J.; Smith, J. N.; Thornton, J. A.; Volkamer, R.; Wang, J.; Worsnop, D. R.; Zaveri, R. A.; Zelenyuk, A.; Zhang, Q. Recent Advances in Understanding Secondary Organic Aerosol: Implications for Global Climate Forcing. Rev. Geophys. 2017, 55, 509–559.
- (22) Riipinen, I.; Yli-juuti, T.; Pierce, J. R.; Petäjä, T.; Worsnop, D. R.; Kulmala, M.; Donahue, N. M. The Contribution of Organics to Atmospheric Nanoparticle Growth. *Nat. Publ. Gr.* 2012, 5, 453–458.
- (23) Kanakidou, M.; Seinfeld, J. H.; Pandis, S. N.; Barnes, I.; Dentener, F. J.; Facchini, M. C.; Van Dingenen, R.; Ervens, B.; Nenes, A.; Nielsen, C. J.; Swietlicki, E.; Putaud, J. P.; Balkanski, Y.; Fuzzi, S.; Horth, J.; Moortgat, G. K.; Winterhalter, R.; Myhre, C. E. L.; Tsigaridis, K.; Vignati, E.; Stephanou, E. G.; Wilson, J. Organic Aerosol and Global Climate Modelling: A Review. Atmos. Chem. Phys. 2005, 5, 1053–1123.
- (24) Nozière, B.; Kalberer, M.; Claeys, M.; Allan, J.; D'Anna, B.; Decesari, S.; Finessi, E.; Glasius, M.; Grgić, I.; Hamilton, J. F.; Hoffmann, T.; Iinuma, Y.; Jaoui, M.; Kahnt, A.; Kampf, C. J.; Kourtchev, I.; Maenhaut, W.; Marsden, N.; Saarikoski, S.; Schnelle-Kreis, J.; Surratt, J. D.; Szidat, S.; Szmigielski, R.; Wisthaler, A. The Molecular Identification of Organic Compounds in the Atmosphere: State of the Art and Challenges. *Chem. Rev.* 2015, 115, 3919–3983.
- (25) Chan, A. W. H.; Isaacman, G.; Wilson, K. R.; Worton, D. R.; Ruehl, C. R.; Nah, T.; Gentner, D. R.; Dallmann, T. R.; Kirchstetter, T. W.; Harley, R. A.; Gilman, J. B.; Kuster, W. C.; de Gouw, J. A.; Offenberg, J. H.; Kleindienst, T. E.; Lin, Y. H.; Rubitschun, C. L.; Surratt, J. D.; Hayes, P. L.; Jimenez, J. L.; Goldstein, A. H. Detailed Chemical Characterization of Unresolved Complex Mixtures in Atmospheric Organics: Insights into Emission Sources, Atmospheric Processing, and Secondary Organic Aerosol Formation. J. Geophys. Res. Atmos. 2013, 118, 6783–6796.
- (26) Camredon, M.; Hamilton, J. F.; Alam, M. S.; Wyche, K. P.; Carr, T.; White, I. R.; Monks, P. S.; Rickard, A. R.; Bloss, W. J. Distribution of Gaseous and Particulate Organic Composition during Dark & alpha; Pinene Ozonolysis. Atmos. Chem. Phys. 2010, 10, 2893–2917.
- (27) Hall IV, W. A.; Johnston, M. V. Oligomer Formation Pathways in Secondary Organic Aerosol from MS and MS/MS Measurements with High Mass Accuracy and Resolving Power. J. Am. Soc. Mass Spectrom. 2012, 23, 1097–1108.
- (28) Meusinger, C.; Dusek, U.; King, S. M.; Holzinger, R.; Rosenørn, T.; Sperlich, P.; Julien, M.; Remaud, G. S.; Bilde, M.; Röckmann, T.; Johnson, M. S. Chemical and Isotopic Composition of Secondary Organic Aerosol Generated by α-Pinene Ozonolysis. *Atmos. Chem. Phys.* 2017, 17, 6373–6391.
- (29) Ziemann, P. J.; Atkinson, R. Kinetics, Products, and Mechanisms of Secondary Organic Aerosol Formation. *Chem. Soc. Rev.* 2012, 41, 6582–6605.
- (30) Carey, F. A.; Sundberg, R. J. Advanced Organic Chemistry: Part A: Structure and Mechanisms; Springer

- Science & Business Media, 2007.
- (31) Gao, S.; Keywood, M.; Ng, N. L.; Surratt, J.; Varutbangkul, V.; Bahreini, R.; Flagan, R. C.; Seinfeld, J. H. Low-Molecular-Weight and Oligomeric Components in Secondary Organic Aerosol from the Ozonolysis of Cycloalkenes and α-Pinene. J. Phys. Chem. A 2004, 108, 10147–10164.
- (32) Yasmeen, F.; Vermeylen, R.; Szmigielski, R.; Iinuma, Y.; Böge, O.; Herrmann, H.; Maenhaut, W.; Claeys, M. Terpenylic Acid and Related Compounds: Precursors for Dimers in Secondary Organic Aerosol from the Ozonolysis of α- and β-Pinene. Atmos. Chem. Phys. 2010, 10, 9383–9392.
- (33) Quirke, J. M. E.; Adams, C. L.; Van Berkel, G. J. Chemical Derivatization for Electrospray Ionization Mass Spectrometry. 1. Alkyl Halides, Alcohols, Phenols, Thiols, and Amines. *Anal. Chem.* 1994, 66, 1302–1315.
- (34) GADDIS, A. M.; ELLIS, R. E. X.; CURRIE, G. T. Girard T Reagent for Carbonyls. *Nature* 1961, 191, 1391–1392.
- (35) Stachissini, A. S.; Do Amaral, L. Kinetics and Mechanism of Benzaldehyde Girard T Hydrazone Formation. *J. Org. Chem.* **1991**, *56*, 1419–1424.
- (36) Mitchel, R. E. J.; Birnboim, H. C. The Use of Girard-T Reagent in a Rapid and Sensitive Method for Measuring Glyoxal and Certain Other α-Dicarbonyl Compounds. *Anal. Biochem.* **1977**, *81*, 47–56.
- (37) Jackson, S. R.; Ham, J. E.; Harrison, J. C.; Wells, J. R. Identification and Quantification of Carbonyl-Containing α-Pinene Ozonolysis Products Using O-Tert-Butylhydroxylamine Hydrochloride. *J. Atmos. Chem.* 2017, 74, 325–338.
- (38) Yu, J.; Griffin, R. J.; Cocker, D. R.; Flagan, R. C.; Seinfeld, J. H.; Blanchard, P. Observation of Gaseous and Particulate Products of Monoterpene Oxidation in Forest Atmospheres. *Geophys. Res. Lett.* 1999, 26, 1145–1148.
- (39) Zhang, X.; McVay, R. C.; Huang, D. D.; Dalleska, N. F.; Aumont, B.; Flagan, R. C.; Seinfeld, J. H. Formation and Evolution of Molecular Products in α-Pinene Secondary Organic Aerosol. *Proc. Natl. Acad. Sci. U. S. A.* 2015, 112, 14168–14173.
- (40) Ma, Y.; Luciani, T.; Porter, R. A.; Russell, A. T.; Johnson, D.; Marston, G. Organic Acid Formation in the Gas-Phase Ozonolysis of α-Pinene. *Phys. Chem. Chem. Phys.* 2007, 9, 5084–5087.
- (41) Johnson, D.; Marston, G. The Gas-Phase Ozonolysis of Unsaturated Volatile Organic Compounds in the Troposphere. Chem. Soc. Rev. 2008, 37, 699–716.
- (42) Aimanant, S.; Ziemann, P. J. Development of Spectrophotometric Methods for the Analysis of Functional Groups in Oxidized Organic Aerosol. *Aerosol Sci. Technol.* 2013, 47, 581–591.
- (43) Tang, I. N.; Fung, K. H.; Imre, D. G.; Munkelwitz, H. R. Phase Transformation and Metastability of Hygroscopic Microparticles. *Aerosol Sci. Technol.* 1995, 23, 443–453.
- (44) Yan, X.; Cheng, H.; Zare, R. N. Two-Phase Reactions in Microdroplets without the Use of Phase-Transfer Catalysts. Angew. Chemie Int. Ed. 2017, 56, 3562–3565.
- (45) Gassin, P.-M.; Girard, L.; Martin-Gassin, G.; Brusselle, D.; Jonchère, A.; Diat, O.; Viñas, C.; Teixidor, F.; Bauduin, P. Surface Activity and Molecular Organization of Metallacarboranes at the Air–Water Interface Revealed by Nonlinear Optics. *Langmuir* 2015, 31, 2297–2303.
- (46) Banerjee, S.; Mazumdar, S. Electrospray Ionization Mass Spectrometry: A Technique to Access the Information

- beyond the Molecular Weight of the Analyte. *Int. J. Anal. Chem.* **2012**, *2012*, 1–40.
- (47) Be, A. G.; Upshur, M. A.; Liu, P.; Martin, S. T.; Geiger, F. M.; Thomson, R. J. Cloud Activation Potentials for Atmospheric α Pinene and β Caryophyllene Ozonolysis Products. 2017.

Reaction Kinetics of Organic Aerosol Studied by Droplet Assisted Ionization: Enhanced Reactivity in Droplets Relative to Bulk Solution

Yao Zhang, Michael J. Apsokardu, Devan E. Kerecman, Marcel Achtenhagen, Murray V. Johnston\*

A brief synopsis: Droplet assisted ionization is used to study the reaction of carbonyl functionalities in secondary organic aerosol (SOA) with Girard's T (GT) reagent, including determination of the second order rate constant and investigation of the effect of inlet temperature, aerosol relative humidity and the presence of salt. Reaction acceleration in droplets is discussed in relation to solvent evaporation and reaction at air-water interface.

